Canadian Journal of Basic and Applied Sciences
©PEARL publication, 2015

ISSN 2292-3381

CJBAS Vol. 03(03), 93-107, March 2015

Automatic Segmentation Of Skin Lesion Using Markov Random Field

Fatemeh Torkashvand, Mehdi Fartash *

Department of Computer Engineering, Arak branch, Islamic Azad University, Arak, Iran.

Keywords:

Inhomogeneities Intensity,
Markov Random Field,
Image segmentation,
Melanoma,
Dermoscopy images

Abstract

The image segmentation is one of the most important topics in the image processing that plays a key role in the image analysis. This study presents a new method to segregate the skin lesions through level set concept with regard to the level of homogeneity and Markov random field. A cluster property with local intensities was extracted from the image during the smoothing and level set phases based on the intensity of heterogeneity and a local clustering function was defined for the intensities of each pixel adjacent to each point. Then, an image is segmented by Markov random field and allocation of each pixel of the image to existing classes that would finally lead to the lesion segregation from the healthy skin. Our method was tested on 200 dermoscopic images taken from the PH^2 database in various color spaces. According to the results and comparison with the results of clinical diagnosis by dermatologists, the proposed method had 94% accuracy in green channel, which indicates a better performance than other color spaces.

1. Introduction

Research has shown that 75 percent of mortality caused by skin diseases results from melanoma [29]. Dermatoscope is an instrument that is used for early diagnosis of melanoma, by which pigment changes in skin lesions in diseases can be assessed. Dermatoscopy is considered as the most common non-invasive method of pigmented and non-pigmented skin lesions based on eye examination [7]. Computer-assisted diagnosis (CAD) systems are developing to accelerate the diagnosis of skin cancer. Computer-assisted diagnosis systems have demonstrated a good performance for the skin lesion pigments in the experimental setting and have accepted at a high level of the affected patients. However, such systems cannot provide the best diagnostic results or replace the skill of physicians or histopathology [7]. Analysis of pigmented skin lesions (PSLs) is an active area of research; one of its main objectives is to develop reliable automatic instruments for diagnosis of skin cancer from the images obtained from the body [7]. Materials and methods for diagnosis of melanoma lesions are clinical screening procedures (by non-dermatologists) and from clinical images, ABCDE criteria [2, 10, 13, 24, 26] and the Glasgow 7-

* Corresponding Author :
E-mail, *m-fartash@iau-arak.ac.ir*

point checklist [24, 27]. At present, diagnosis through only computer-assisted systems based on PSL image analysis cannot be used to provide the best diagnostic results. Furthermore, a lack of benchmark data for evaluation of standardized algorithm is a barrier to a more dynamic development of this research area [7]. Thus, it is of high importance to detect borders of a skin lesion accurately so that the disease can be diagnosed automatically. Therefore, border detection is one of the most important areas in the computerized analysis of PSLs [3, 5, 7, 9]. Morphological structure of a lesion acts as a misleading factor for both manual and automatic segmentation [7]. These problems have led to the development of a wide variety of PSL segmentation methods that are as wide as the categorization of all segmented algorithms [7]. One method for detection of skin pigments is to use dermoscopy images of automatic edge diagnosis for differentiation of the lesion from the skin. Errors play a key role in automatic segmentation and thus they must be minimized and then the figure specifications must be extracted from this edge [2].

At present, CAD systems cannot provide the best diagnostic results or replace the dermatologists [7]. Many articles of the classification of skin images have automatically used the ABCD rule (asymmetry, border irregularity, different colors, and diameter > 6 mm) [2, 7, 10, 13]. In general, one or a combination of the existing rules in ABCD has been used to diagnose the lesions in the published articles [3, 5, 9, 10, 13, 24]. Wang et al. [1] could divide the skin lesions with a high accuracy through watershed based algorithm.

Situ et al. [8] provided a developed ES-based segmentation technique for automatic division of the skin lesion images. The technique did not need to give input parameters, such as threshold and their performance did not depend on initial values. Dalal et al. [6] obtained an adaptive detection method to detect white and hypopigmented areas based on the lesion histogram statistics. They segmented the lesion in concentric deciles via Euclidean distance conversion. Isasi al. (2011) introduced a method based on standard ABCD rule and diagnostic protocols of skin patterns .They also developed a complete stack of algorithms for asymmetry, border, color, and parameter of diameter [10]. Capdehourat et al. [2] proposed a learning machine approach to classify melanocytic lesions via dermoscopic images. They performed the learning and classification stages through AdaBoost with C4.5 decision trees. Sadeghi, et al. [11] introduced a graph-based method for the classification of skin pigments. Ruiz et al. [13] introduced the use of a decision support system clinical for the diagnosis of melanoma through individual distinct classification methods with a common method. This logic was based on the first phase of process and segmentation using Otsu threshold method. They conducted three methods for the classification of images obtained from skin lesions: K algorithm of the closest neighbor, Bayesian classification, and a multilayered perceptron.

This system makes the segmentation of lesion into two benign and melanoma groups possible. Panjwani et al. [30] developed the MRF model for unsupervised segmentation of the color images of tissue. Serrano et al. [14] used the MRF model to detect dermoscopic image patterns in terms of apparent color of these patterns. Here, the analysis was based on various color patterns in the skin lesions rather than on instead of detection of characteristics, including border irregularities, color or other tissue characteristics. They aimed to classify 40×40 pixels images into probable patterns that should allocate all images to a specific label. This paper presented a new method to classify dermoscopic images, which can be also applied on lesions with intense heterogeneities. A local clustering property has been derived and a criterion function has been defined for local clustering in one point of each area. The local clustering criterion has integrated more than one area adjacent the center and has transformed into a level set formula. After the operation of smoothing the lesion level, Markov Random Field was used for detection of the lesion or differentiation of the lesion from the healthy skin, which is the purpose of the paper. The Markov theory provides an appropriate and compatible solution for modeling the image pixels and the related properties. The present paper is organized into the following sections:

The proposed method is discussed in section two. Section three presents the laboratory results of the proposed method and section four deals with the results.

2. Proposed method

Fig.1 presents the flowchart of the Markov Random Field algorithm explored in this study. Each individual component will be discussed in following sections.

The presented method is a proposal for the differentiation of skin lesion from the background skin. The method was used due to the simplicity and reduction in the used energy for diagnosis.

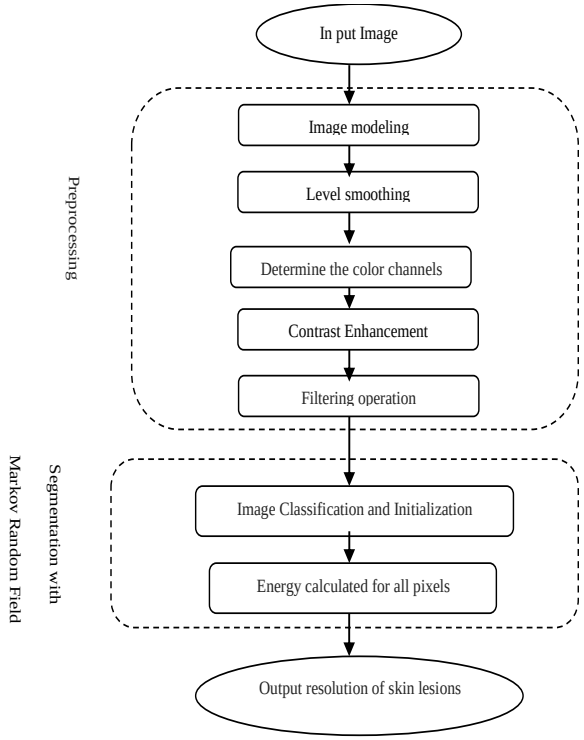

Figure 1. flowchart of the proposed method

2.1. Pre- processing

This section considered the pre-processing process, which facilitates the lesion diagnosis.

2.1.1. Image modeling

Intense heterogeneity is a challenging problem in the image segmentation.

The level set method, originally used as numerical techniques for figures, has been increasingly used to segment the images in the past decades. With the level set representation, the image segmentation problem can be well-established through formulation and a systematic problem-solving based on mathematical theories. Therefore, a feature of local clustering has been derived and a criterion function has been defined for local clustering in a point of each area. The local clustering criterion has integrated more than one area adjacent the center that was transformed into a level set formula. An observed image I can be modeled as [31] :

$$I = bJ + n \tag{1}$$

where J is the true image, b is a component that accounts for the intensity of heterogeneity, which changes slowly and n is the added noise. Image I has been considered as a function $I: \Omega \to \mathbb{R}$, which has been defined on a continuous domain Ω. Assumptions about the true image J and the bias field b can be stated more specifically as follows:

1) The bias field b changes slowly implying that b can be well approximated by a constant in neighborhood of each point in the image domain

2) The true image J is approximated with N distinct constant values $C_1, \dots, C_N$ in discontinuous areas $\Omega_1, \dots, \Omega_N$, respectively, where $\{\Omega_i\}_{i=1}^N$ is in a form of a partition of the image domain [31].

According to the above-mentioned equation (1) and cases (1) and (2), we proposed a method to estimate the areas $\{\Omega_i\}_{i=1}^N$, constants $\{C_i\}_{i=1}^N$, and bias field b. The estimates obtained from them with $\{\hat{\Omega}_i\}_{i=1}^N$, the constants $\{\hat{C}_\iota\}_{i=1}^N$, and bias field b respectively should slowly change and the areas $\hat{\Omega}_1, \dots, \hat{\Omega}_N$ should satisfy certain regular property to avoid spurious segmentation results caused by image noise.

We considered an adjacent circle with a radius M at the center of each point y ∈ Ω that has been defined by $O_y \triangleq \{X: |x - y| \leq \rho\}$. The partitioning $\{\Omega_i\}_{i=1}^N$ of the entire domain Ω induced a partitioning adjacent to O_y. For a slow change in bias field b, the values $b(x)$ for all X in the neighborhood of circle O_y are almost equal to $b(y)$.

For instance, $b(x) \approx b(y)$ is for $x \in O_y$. Thus, the intensities $b(x)J(x)$ in each initial segmentation of area $O_y \in \Omega_i$ has been close to the constant $b(y)C_i$. Considering the image model in equation (1), we therefore have [31]:

$$I(x) \approx b(y)C_i + n(x)$$

Where $x \in O_y \cap \Omega_i$ and $n(x)$ are additive zero-mean Gaussian noise. Therefore, the intensity in the set $I_y^i = \{I(x): x \in O_y \cap \Omega_i\}$ forms a cluster with the central cluster $m_i \approx b(y)C_i$, which can be considered as the samples drawn from a Gaussian distribution with mean $\mathrm{m_i}$. It is clear that the N clusters $I_y^1, \dots, I_y^N$ with distinct cluster centers $C_1, \dots, C_N$ have been well-separated from each other because the constants $C_1, \dots, C_N$ are distinct and the variance has been considered from n Gaussian noise that is relatively small. The above-mentioned local intensity clustering property allows us to apply the standard K-means clustering to classify the local intensity [31].

The clustering criterion for classification of intensity in O_y is defined as

$$\varepsilon_y = \sum_{i=1}^N \int_{\Omega_i \cap O_y} k(y - x)|I(x) - b(y)C_i|^2 \, dx \quad (2)$$

Where $k(y - x)$ is introduced as a nonnegative function and is called kernel function, such that $k(y - x) = 0$ for $x \notin O_y$. According to the equation (2), the clustering criterion function ε_y can be rewritten as:

$$\varepsilon_y = \sum_{i=1}^N \int_{\Omega_i} k(y - x)|I(x) - b(y)C_i|^2 \, dx \quad (3)$$

This local clustering criterion function is a basic element in the formulation of the presented method.

2.1.2. Level smoothing

A simple implementation was used to smooth the level that would greatly reduce the computational cost and was significantly faster. In numerical implementation, the Heaviside function *H* is a smooth function that approximates *H* called the smoothed Heaviside function H_ϵ , which is replaced by [31,32]:

$$H_\epsilon(x) = \frac{1}{2}\left[1 + \frac{2}{\pi}\, arctan\left(\frac{x}{\epsilon}\right)\right] \quad (4)$$

In this equation, ϵ*=1*.

Accordingly, in delta structure δ , which is the derivative of the Heaviside function *H*, it is replaced and computed by the derivative of H_ϵ, which is by

$$\delta_\epsilon(x) = H'_\epsilon(x) = \frac{1}{\pi}\frac{\epsilon}{\epsilon^2 + x^2} \quad (5)$$

In each time phase, the constant $C = (C_i, \dots C_N)$ and the bias field b could be updated according to the following equation:

$$\widehat{C_\iota} = \frac{\int (b * k) I u_i \, dy}{\int (b^2 * k) u_i \, dy} \;, i = 1, \dots, N \quad (6)$$

Where $u_i(y) = M_i\big(\emptyset(y)\big)$

$$\hat{b} = \frac{(IJ^{(1)}) * k}{J^{(2)} * k} \quad (7)$$

In the above equation, $J^{(1)} = \sum_{i=1}^{N} C_i u_i$ and $J^{(2)} = \sum_{i=1}^{N} {C_i}^2 {u_i}^2$.

Parameter δ and its size adjacent to O_y that has been specified by radius ρ should be relatively smaller for images with more localized intensity heterogeneity.

Thus, the smoothing operation is applied on the images [31, 32].

Table 1. The color channels used in changing the color spaces

Color paces	Color channels
RGB	R, G, B, R&B&G
XYZ	X, Y, Z, X&Y&Z, X&Z, X&Y, Y&Z
HSV	H, S, V
GARAY	GARAY
LAB	L, A, B
YIQ	Y , I, Q

2.1.3. Determine the color channels

Color information plays a significant role in the analysis of dermoscopic image. Color channels use various spaces to maximize the discrimination between lesion and healthy skin [9]. The RGB image can be used directly or it might be transformed into a different color space for various reasons including: (i) reducing the number of channels, (ii) decoupling luminance and chromaticity information, (iii) ensuring approximate perceptual uniformity, and (iv)achieving invariance to

different imaging conditions such as viewing direction, illumination intensity, and highlights [3]. Colorful canals enjoy various spaces to minimize the contrast between the lesion and the healthy skin. Using the luminance transformation, chromaticity and color information of an RGB image can be calculated. for example:

$$\text{Luminance} = 0.395 \times \text{R} + 0.763 \times \text{G} + 0.216 \times \text{B}$$

This phase includes information of the dermoscopy image color, in which the original image has been transformed into the studied color channels. The following color spaces have been investigated in this paper:

RGB, XYZ, HSV, LAB, Garay,YIQ

Dermoscopic images have been transformed into a set of color channels of the above-mentioned color spaces. (In this study lesions are often more prominent in green channel).

As shown in Table 1, these images include a single color channel, such as R from the RGB color space and H from the HVS color space, as well as a combination of them, such as R & G & B, where "&" stands for logical AND in order to combine the R,G,B color channels from the RGB color space.

2.1.4. Contrast enhancement

Images with low contrast often are created due to the poor lighting. The contrast enhancement of images is performed by a register of input image intensity values to new values. Such a contrast enhancement in images by transformation of the intensity of the values of an image is done in a way that histogram of the output image has been nearly determined such as the histogram. Contrast can be determined to avoid the increased noise that may exist. Some images may lack the sufficient resolution so their contrast should be increased**.**

2.1.5. Filtering operation

To enhance the accuracy of segmentation and save computational time, it is used to eliminate the artificial traces, such as skin lines, air bubbles or other noises caused by the imaging process [9]. In this study, Gaussian filter will cause the low image frequencies to remain in the filtered image. The filter possesses two inputs. The first one determines the size of the filter network and the second determines the amount of filter frequency.

$$h_g(n_1, n_2) = e^{-\frac{n_1^2+n_2^2}{2\sigma^2}}$$

$$h(n_1, n_2) = \frac{h_g(n_1, n_2)}{\sum_{n_1}\sum_{n_2} h_g}$$

2.2. Markov Random Field for Lesion segmentation

Markov random field enjoys the concept of batch (one pixel and the set of neighbors) and Gibbs distribution for the image segmentation. In Markov random field-based methods, the purpose is to minimize the energy function in order to achieve an ideal segmentation. Performance of Markov random field in classifying dermoscopic images is as follows:

The classification is in the form of a question of incomplete data, in which the value of each pixel is recognized and labeled. After the pre-processing operation on dermoscopic images, the pixels with values of -1, 0, and 1 are labeled. While diagnosing the lesion with Markov random field if the pixel is X>0, 1 would be assigned to the pixels and if the pixel is X≤0, -1 would be assigned to the pixels. In this technique, the image areas are modeled and considered as random background. The main purpose of segmentation with Markov random field is to minimize the energy function or the probable allocation of one pixel to one class.

2.2.1.Image Classification and Initialization

Using Maximum A Post Priority (MAP) it is possible to calculate the possible allocation of each image pixel to different existing classes. Therefore, the class of each real X image pixels would be chosen in a way that P(Y|X) is maximized. Y is a preliminary estimation of pixel classes X and $\hat{Y}$ is the Matrix of real X pixels class.

$$\hat{Y} = \text{argmax}P(Y|X) \tag{8}$$

$$P(Y|X) = \frac{P(X|Y)P(Y)}{P(X)} \tag{9}$$

According to the Bayse relation and assuming the possible equality for all light intensity quantities in each pixel (as a preliminary option), the possible P(X) is neglected and is rewritten as follows:

$$P(Y|X) \propto P(X|Y)P(Y) \tag{10}$$

2.2.2. Energy calculated for all pixels

To express the possible different quantity of the pixels' light intensity on the basis of which classes it may be belong($P(X|Y)$), various distributions can be used. However, the Gaussian distribution is used with the assumption of the existence of Gaussian noise in images. Therefore, the possibility of pixel light intensity i with the assumption of belonging to class y_i is equal to x_i would be calculated as follows (x_i and y_i are each element of matrices X and Y):

$$P(x_i|y_i) = \frac{1}{\sqrt{2\pi\sigma_{y_i}}} \exp\left\{-\frac{\left(x_i-\mu_{y_i}\right)^2}{2\pi{\sigma_{y_i}}^2}\right\} \quad (11)$$

$$P(X|Y) = \prod_{i=1}^{MN} P(x_i|y_i)$$

$$= \prod_{i=1}^{MN} \frac{1}{\sqrt{2\pi\sigma_{y_i}}} \exp\left\{-\frac{\left(x_i-\mu_{y_i}\right)^2}{2\pi{\sigma_{y_i}}^2}\right\} \quad (12)$$

μ_{y_i}, σ_{y_i} in the above relations indicate respectively the mean and variance of the class members y_i. This is because Y is a Markov segregated random field. According to the equation (10):

$$P(X_i|Y_i = y) \propto \frac{1}{\sqrt{2\pi\sigma_{y_i}}} \exp\left(-\frac{\left(x_i-\mu_{y_i}\right)^2}{2\pi{\sigma_{y_i}}^2}\right) \times \frac{1}{z} \exp\left(-\frac{1}{T}\sum_{c\in C}^{y_i} V_c(y_i)\right) \quad (13)$$

Logarithm of the equation sides and deletion of constant values give the following equation:

$$E = \frac{1}{2}\ln\left({\sigma_{y_i}}^2\right) + \frac{\left(x_i-\mu_{y_i}\right)^2}{2{\sigma_{y_i}}^2} + a\sum_{c\in C} V_c(y_i) \quad (14)$$

The above equation is defined as energy function.

In the above equation, we have $a = \frac{1}{T}$. Since the above function is logarithmic and the obtained possibilities have an exponential form, the logarithm can be maximized; consequently the following equation would be resulted:

$$\hat{y}_i = \text{argmin}P(x_i|y_i) \quad (15)$$

The main goal of the dermoscopic image segmentation through Markov random field is to minimize the energy function or maximize the possibility of belonging of one pixel to a class, which is obtained by changing different parameters. Using the repetitive methods, equation (15) can be answered.

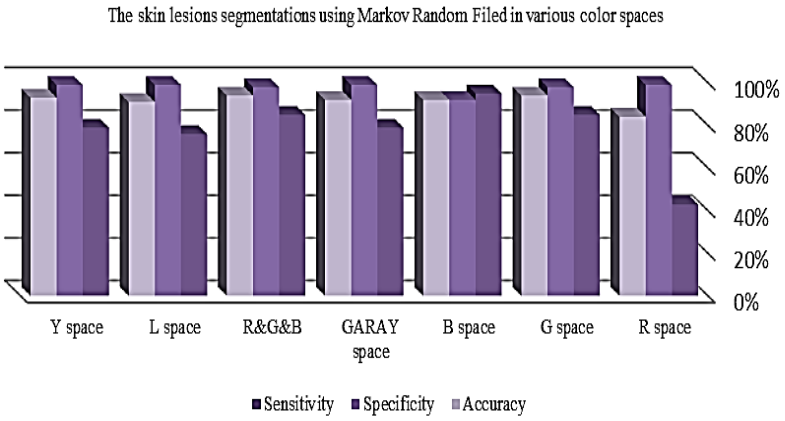

Figure 2. the obtained results from various color areas

3. Experimental results

During the present research project, a dermoscopic image bank named PH2 was investigated.The PH2 database has been obtained by joint research collaboration between Lisbon University and dermatologists of Hispano hospital in Portugal. The PH2 database consists of manual segmentation, clinical diagnosis, and definition of several dermoscopic structure displayed by experienced dermatologists. The database of a set of 200 melanocytic images contains 80 common nevi, 80 atypical nevi, and 40 melanomas. The activities in Hispano hospital have been done for clinical diagnosis. The features obtained from clinical diagnosis were evaluated by dermoscopic features in clinical methods, such as ABCD rule, the 7-point checklist and the Menzies methods that are widely used [24]. In this database, the lesions were first manually obtained by dermatologists. The results of the proposed algorithm were compared with the lesions that have been obtained manually by dermatologists. To perform the comparison, three different criteria were evaluated that are sensitivity (equation (16)), specificity (equation (17)), and accuracy (equation (18)) [3,9] .

$$\text{Sensitivity} = \frac{TP}{TP+FN} \times 100 \quad (16)$$

$$\text{Specificity} = \frac{TN}{TN+FP} \times 100 \quad (17)$$

$$\text{Accuracy} = \frac{\text{TP+TN}}{\text{TP+FP+FN+TN}} \times 100 \quad (18)$$

Where TP, TN, FP and FN refer to true positive, true negative, false positive, and false negative, respectively. TP and TN respectively represent the number of pixels, which are as a part of the lesion and background skin for both the manual and automatic classification. FP represents the number of pixels, which is automatically classified as a part of lesion in the border but is labeled as a part of the background skin in the manual border of lesion. Finally, FN represents the number of pixels, which is automatically classified as a part of the background skin in the border but is labeled as a part of the lesion in the manual border [3, 9].

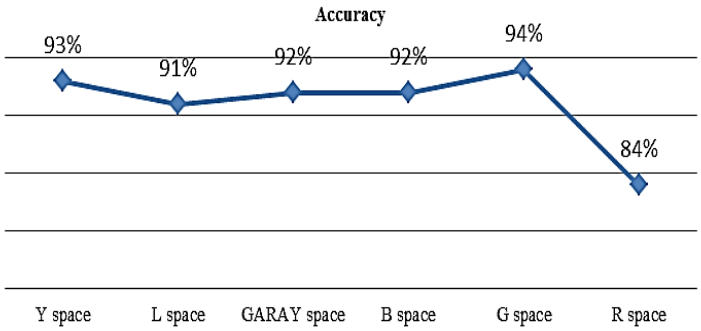

Figure 3. Accuracy in different color spaces

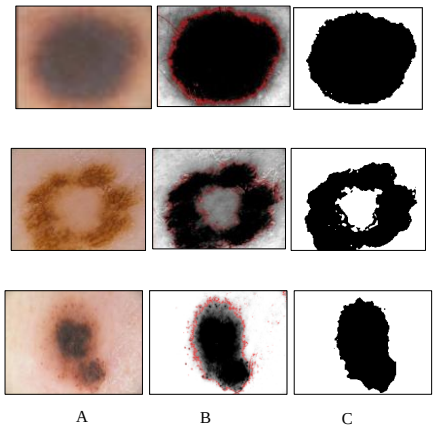

Figure 4. A: original image, B: healthy skin and lesion in the preprocessing phase, C: the lesion obtained by removing the surrounding healthy skin.

The proposed method is applied on the dermoscopic images as follows:

After the smoothing level operation on the lesion levels in dermoscopic images and initializing bias field during smoothing, the pixels comprising the lesions will be as follows:

If pixel is x>0, then the value would be 1.

If pixel is x=0, then the value would be 0.

And if pixel is x<0, then the value -1 would be considered for the initialization of bias field. According to this initialization and allocation of each pixel to any of the above values, the lesion and healthy skin are gradually differentiated. Then, the existing artifacts around the lesion are removed by the filtering operation and the segmentation operation would be performed by Markov random field in order to give the final diagnosis of lesion with normalization of image in a range (1,-1).Figure 4 shows phases of the proposed method.

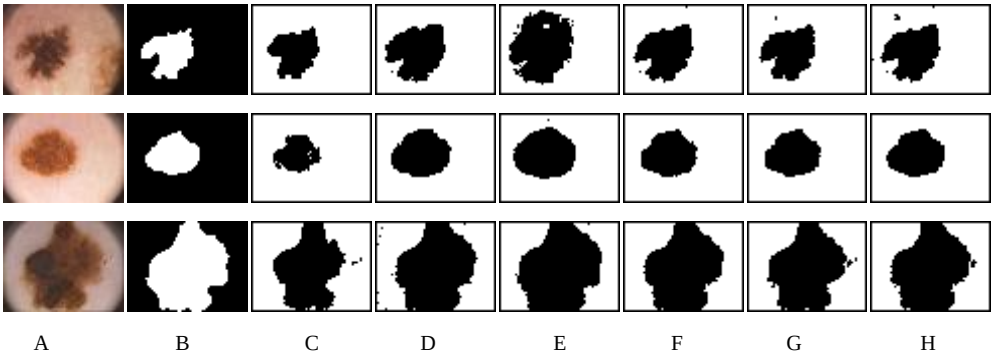

Figure 5. A: original image, B: detection of lesion by dermatologists, C: detection of lesions in the color channel R, D: detection of lesions in the color channel G, E: detection of lesion in the color channel B, F: detection of lesion in the color space GARAY, G: detection of lesion in color channel L, H: detection of lesion in color channel Y

The method proposed on this database was studied in six color spaces XYZ, HSV, LAB, YIQ, GARAY, and RGB. Table 2 presents results obtained from the color spaces compared with manual diagnosis done by dermatologists:

Table 2. Results of detection of skin lesions through Markov random fields in some color channels

The skin lesions segmentations using Markov random filed in various color spaces							
	R space	G space	B space	GARAY space	R&G&B	L space	Y space
Sensitivity	43%	85%	95%	79%	85%	76%	79%
Specificity	99%	98%	92%	99%	98%	99%	99%
Accuracy	84%	94%	92%	92%	94%	91%	93%

4.Conclusion

In this study, the skin lesions were detected and the lesion was segregated from the healthy skin through Markov random field. The main goal of the image segmentation through Markov random fields was to minimize the energy function or to maximize the probability of pixel allocation to a cluster. To facilitate the process of segmentation, a preprocessing was first done on the images before using the concept of Markov random field. Dermoscopic images with a resolution of 768 *560 pixels were studied by the PH2 database. To cope with the roughness in images, a level set function was used to smooth the images. Then, parameters of accuracy, specificity, and sensitivity

were calculated by Markov random field in the final diagnosis of lesion in color spaces XYZ, HSV, LAB, YIQ, GARAY, RGB.

According to the obtained results and comparing them with that of clinical diagnosis results by dermatologists, the proposed method had 94% accuracy in color space of R&G&B and G channel and 93% accuracy in Y color channel, which showed a better performance than other color spaces.

References

[1] Wang H., Moss R. H., Chen X., Stanley R. J., Stoecker W. V., Celebi M. E., Szalapski T. M.: Modified watershed technique and post-processing for segmentation of skin lesions in dermoscopy images. Computerized Medical Imaging and Graphics, **35**, 116–120 (2011).

[2] Capdehourat G., Corez A., Bazzano A., Alonso R., Musé P.: Toward a combined tool to assist dermatologists in melanoma detection from dermoscopic images of pigmented skin lesions. Pattern Recognition Letters, **32**, 2187–2196 (2011).

[3] Celebi M. E., Iyatomi H., Schaefer G., Stoecker W. V.: Lesion border detection in dermoscopy images. Computerized Medical Imaging and Graphics, **33**, 148–153 (2009).

[4] Zhou H., Schaefer G., Celebi M. E., Lin F., Liu T.: Gradient vector flow with mean shift for skin lesion segmentation. Computerized Medical Imaging and Graphics, **35**, 121–127 (2011).

[5] Schaefer G., Rajab M. I., Celebi M. E., Iyatomi H.: Colour and contrast enhancement for improved skin lesion segmentation. Computerized Medical Imaging and Graphics, **35**, 99–104 (2011).

[6] Dalal A., Moss R. H., Stanley R. J., Stoecker W. V., Gupta K., Calcara D. A., Perry L. A.: Concentric decile segmentation of white and hypopigmented areas in dermoscopy images of skin lesions allows discrimination of malignant melanoma. Computerized Medical Imaging and Graphics, **35**, 148–154 (2011).

[7] Korotkov K., Garcia R.: Computerized analysis of pigmented skin lesions: a review. Artificial Intelligence in Medicine, **56**, 69–90 (2012).

[8] Situ N., Yuan X., Mullani N., Zouridakis, G.: Automatic segmentation of lesion images using evolutionary stratge. Biomedical Signal Processing and Control, **3**, 220–228 (2008).

[9] Garnavi R., Aldeen M., Celebi M. E., Varigos G., Finch S.: Border detection in dermoscopy images using hybrid thresholding on optimized color channels. Computerized Medical Imaging and Graphics, **35**, 105–115 (2011).

[10] Isasi A. G., Zapirain B. G., Zorrilla A. M.: Melanomas non-invasive diagnosis application based on the ABCD rule and pattern recognition image processing algorithms. Computers in Biology and Medicine, **41**, 742–755 (2011).

[11] Sadeghi M., Razmara M., Lee T. K., Atkins M. S.: A novel method for detection of pigment network in dermoscopic images using graphs. Comput Med Imaging Gragh, **35**, 137–143 (2011).

[12] Iyatomi H., Celebi M. E., Schaefer G., Tanaka M.: Automated color calibration method for dermoscopy images. Computerized Medical Imaging and Graphics, **35**, 89–98 (2011).

[13] Ruiz D., Berenguer V., Soriano A., Sánchez B.: A decision support system for the diagnosis of melanoma: A comparative approach. Expert Systems with Applications, **38**, 15217–15223 (2011).

[14] Serrano C., Acha B.: Pattern analysis of dermoscopic images based on Markov randomfields. Pattern Recognition, **42**, 1052 -1057 (2009).

[15] Zhou Y., Smith M., Smith L., Farooq A., Warr R.: Enhanced 3D curvature pattern and melanoma diagnosis. Comput Med Imaging Gragh, **35**, 155–165 (2011).

[16] Barata C., Ruela M., Francisco M., Mendonça T., Marques J. S.: Two systems for the detection of melanomas in dermoscopy images using texture and color features. Systems Journal, IEEE, : 1-15 (2013).

[17] Barata C., Marques J. S., Mendonça T.: Bag-of-Features classification model for the diagnose of melanoma in dermoscopy images using color and texture descriptors. Image Analysis and Recognition, **7950**, 547-555 (2013).

[18] Thon K., Rue H., Skrøvsetha S. O., Godtliebsen F.: Bayesian multiscale analysis of images modeled as Gaussian Markov random fields. Computational Statistics & Data Analysis, **56**, 49-61 (2012).

[19] Barata C., Marques J. S., Rozeira J.: The role of keypoint sampling on the classification of melanomas in dermoscopy images using Bag-of-Features. Pattern Recognition and Image Analysis, **7887**, 715-723 (2013).

[20] Barata C., Marques J. S., Rozeira J.: A System for the detection of pigment network in dermoscopy images using directional filters. Biomedical Engineering, IEEE Transactions, **59**, 2744 – 2754 (2012).

[21] Ferreira P. M., Mendonca T., Rocha P.: A wide spread of algorithms for automatic segmentation of dermoscopic images. Pattern Recognition and Image Analysis, **7887**, 592-599 (2013).

[22] Silveira M., Nascimento J. C., Marques J. S., Marcal A. R. S., Mendonca T., Yamauchi S., Rozeira, J.: Comparison of segmentation methods for melanoma diagnosis in dermoscopy images. Selected Topics in Signal Processing, IEEE Journal, **3**, 35-45 (2009).

[23] Ayoub A., Hajdu A., Nagy A.: Automatic detection of pigmented network in melanoma dermoscopic images. The International Journal of Computer Science and Communication Security, **2**, 58-63 (2012).

[24] Mendonca T., Ferreira P. M., Marques J. S., Marcal A. R. S., Rozeira J.: PH2- A dermoscopic image database for research and benchmarking, 5437 – 5440 (2013).

[25] Dobrescu R., Dobrescu M., Mocanu S., Popescu D.: Medical images classification for skin cancer diagnosis based on combined texture and fractal analysis. Wseas Transactions on Biology and Biomedicine, **7**, 223-232 (2010).

[26] Abbasi N. R., Shaw H. M., Rigel D. S., Friedman R. J., McCarthy W. H.: Early diagnosis of cutaneous melanoma: revisiting the ABCD criteria. The Journal of the American Medical Association, **292**, 2771-2776 (2004).

[27] Argenziano G., Catricala C., Ardigo M., Buccini P., Simone P., Eibenschutz L., Zalaudek I.: Seven-point checklist of dermoscopy revisited. British Journal of Dermatology, **164**, 785–790 (2011).

[28] Berenguer V. J., Ruiz D., Soriano, A.: Application of hidden markov models to melanoma diagnosis. International Symposium on Distributed Computing and Artificial Intelligence 2008 (DCAI 2008), **50**, 357-365 (2009).

[29] Rigel D. S., Russak J., Friedman R.: The evolution of melanoma diagnosis: 25 years beyond the ABCDs. CA Cancer J Clin, **60**, 301–316 (2010).

[30] Panjwani D. K., Healey G.: Markov random field models for unsupervised segmentation of textured color images. Pattern Analysis and Machine Intelligence, IEEE Transactions on, **17**, 939 – 954 (1995).

[31] Li C., Huang R., Ding Z., Gatenby J. C., Metaxas D. N.: A Level set method for image segmentation in the presence of intensity inhomogeneities with application to MRI. Image Processing, IEEE Transactions on, **20**, 2007 – 2016 (2011).

[32] Li C., Kao C. Y., Gore J. C., Ding Z.: Minimization of region-scalable fitting energy for image segmentation. IEEE Transactions on Image Processing, **17**, 1940-1949 (2008).